Guiding Light Through Sharp Bends Using Two Dimensional Photonic Crystals

Personnel
S. Assefa, A. A. Erchak, D. J. Ripin, S. G. Johnson, M. Mondol, G. S. Petrich, E. P. Ippen, J. D. Joannopoulos, H. I. Smith and L. A. Kolodziejski

Sponsorship
NSF

The current effort to make integrated optical chips requires guiding light around sharp corners with a radius of curvature on the order of a wavelength. Light propagates in conventional waveguides as a result of total internal reflection at the interface between the high-refractive index guiding layer and its low-index surroundings. However, bends in the conventional index-contrast waveguides are susceptible to large optical losses depending on the radius of curvature of the bend. These optical losses, due to radiation, can be avoided by using a Two-Dimensional (2D) photonic crystal.

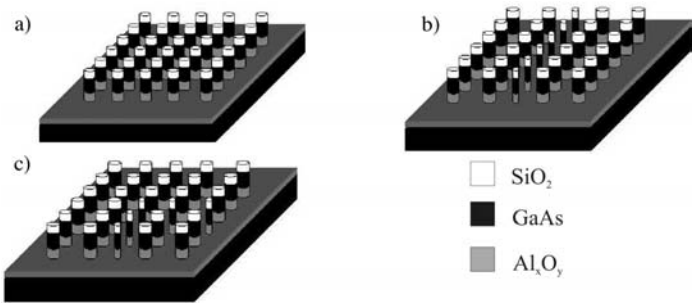

Fig. 10: a) A photonic crystal. b) A linear waveguide consisting of cylinders with a smaller diameter within a photonic crystal. c) A 90º bend in the waveguide embedded in the photonic crystal.

The 2D photonic crystal consists of a periodic array of cylindrical rods of high dielectric material residing on a low dielectric material. Introducing a line defect, such as a row of cylinders with a different radius, into the 2D photonic crystal results in a linear waveguide. The radius of the cylinders in the line defect remains large enough to provide index guiding in the vertical dimension (normal to the plane of periodicity). The periodic arrangement of dielectric rods surrounding the line defect creates a Photonic Band Gap (PBG) i.e. a range of frequencies in which light cannot propagate. Thus, an optical signal with a frequency within the PBG has its energy confined in the line defect and evanescently decays into the photonic crystal. The localization of a mode inside the line defect can be utilized to guide light around sharp corners including a 90º bend with low optical loss. Figure 10 shows a photonic crystal (a), a linear waveguide consisting of cylinders with a smaller diameter within a photonic crystal (b) and a 90º bend within the photonic crystal (c).

The cylindrical rods of the photonic crystal consist of a high-index, 860 nm thick epitaxial layer of GaAs between a 300 nm thick SiO_2 cap layer and a 640 nm thick low-index Al_xO_y layer. An additional 860 nm thick Al_xO_y layer resides below the cylindrical rods in order to isolate the GaAs guiding layer from the GaAs substrate. The heterostructure is grown using gas source molecular beam epitaxy on a (100) GaAs substrate. The Al_xO_y is initially grown epitaxially as AlGaAs.

The fabrication process commences by sputtering a 300 nm thick SiO_2 layer on the sample using the sputtering system within the NanoStructures Laboratory (NSL). Next, the waveguide and photonic crystal are defined by using direct-write electron-beam lithography. Each sample is coated with PolyMethyl MethAcrylate (PMMA) electron-beam resist. Although each cylinder is defined by exposing a square pattern, the finite width of the beam rounds-off the corners of each square yielding a circular hole upon development. Simulations show that the largest band gap is obtained from a periodic arrangement of rods with a diameter of 300 nm. To observe a shift in the frequency range of the PBG, photonic crystals with cylinder diameters ranging from 270 nm to 330 nm are fabricated. Exposure-dose experiments are done to find the optimal parameters for the exposures. As shown in Figure 11, a dose of 375 $\mu C/cm^2$, current of 50 pA, and clock frequency of 0.09 MHz yield hole diameters close to the desired values. The input and output coupling waveguides and different sized arrays of holes are written by stitching 250 µm fields together.

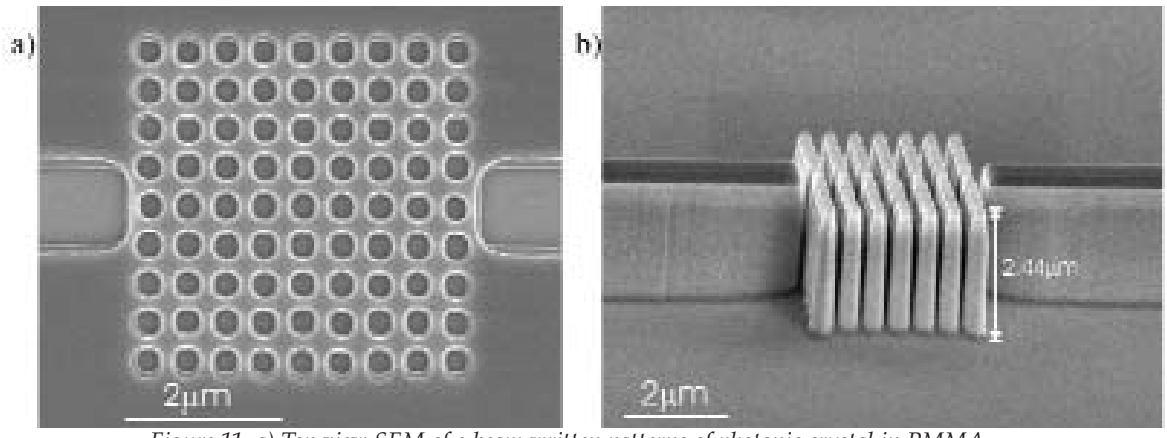

Figure 11. a) Top view SEM of e-beam written patterns of photonic crystal in PMMA. b) Side view SEM of a photonic crystal etched in GaAs using BCl_3 plasma.

Using the NSL electron beam evaporator, a 50 nm thick film of nickel is evaporated on the sample after the PMMA is developed, and a liftoff process is performed. The pattern is transferred to the SiO_2 using the NSL Reactive-Ion Etcher (RIE) with a CHF_3 plasma, after which a nickel etchant is used to remove the nickel mask. Using the patterned SiO_2 layer as a hard mask, the cylindrical rods are created by etching the GaAs and the AlGaAs to a total depth of 1.5 µm in a BCl_3 plasma. During the BCl_3 etch, the power and the DC bias are carefully monitored to control the etch rate and to avoid sputtering the SiO_2 mask, hence eliminating micromasking. Also, the etching is done at low pressure and low flow to minimize the formation and excessive deposition of polymers on the mask and the waveguide sidewalls. As more material is etched, the aspect ratio of the cylinders increases; lowering the BCl_3 flow minimizes microloading by increasing the number of radicals and ions available at the surface of the sample. This etching process leaves behind approximately 250 nm of the SiO_2 mask. Next, the AlGaAs is transformed into Al_xO_y using a wet thermal oxidation process. Finally, each substrate is lapped and the sample is cleaved in order to create a smooth input facet to promote the efficient coupling of a test signal with a wavelength of 1.55 µm.

The fabrication of the 2D photonic crystal waveguide structures is near its completion. Different configurations of input and output coupling waveguides are currently under investigation in an effort to minimize coupling loss due to reflections at the edge of the photonic crystal. One configuration under investigation is shown in Figure 12. The input waveguide is inserted into the photonic crystal and tapered to a width of 300 nm. The output waveguide is inverse-tapered and also starts inside the photonic crystal.

In the near future, transmission through the various structures will be measured. Of particular interest is the size of the photonic bandgap and the transmission through a line defect waveguide. Coupling losses at the input and output of the 2D photonic crystal waveguide will be investigated. Finally, the transmission through a sharp 90° bend will be measured and compared to theoretical simulations.

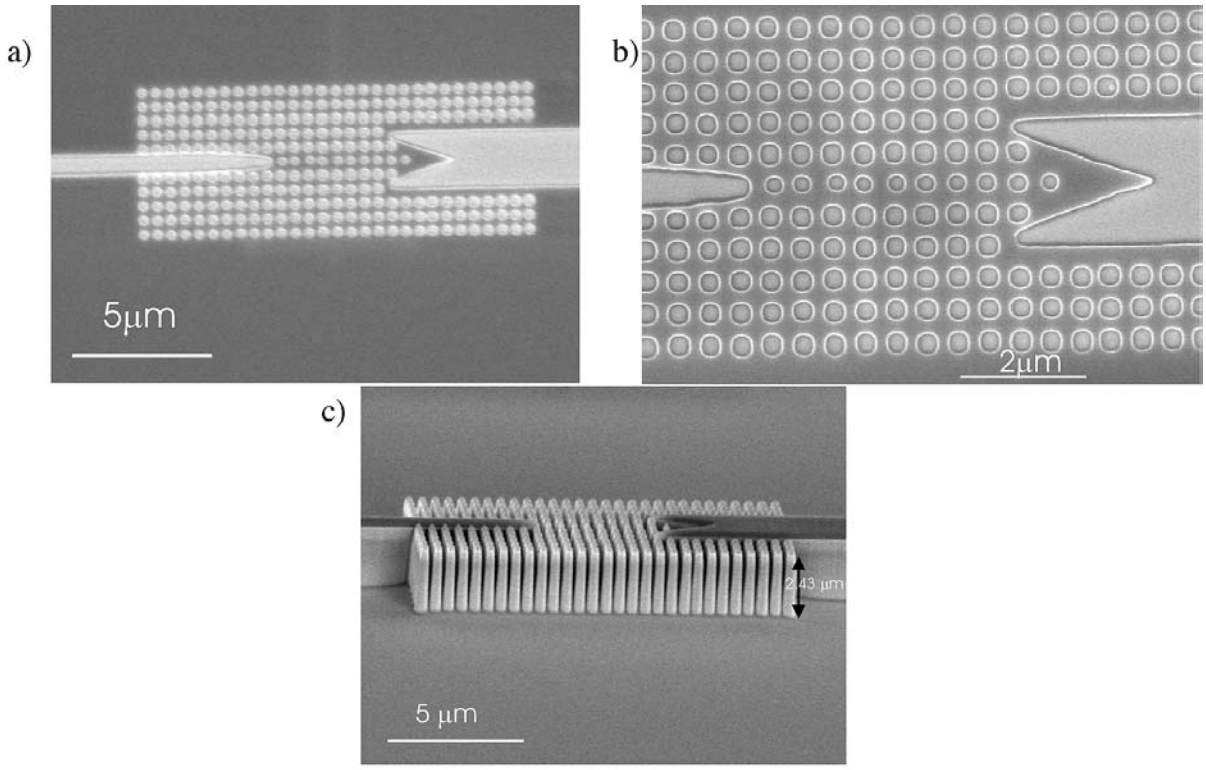

Fig. 12: a) Plan view SEM micrograph of an electron-beam written linear-defect with tapered input and output coupling waveguides in PMMA. b) Magnified view of the line-defect waveguide with tapered input and output waveguides in PMMA. c) Side view SEM micrograph of same design after pattern transfer into GaAs using a BCl_3 plasma.